Proc. 31st Int. Workshop on Vertex Detectors (VERTEX2022)
JPS Conf. Proc. **42**, 011023 (2024)
https://doi.org/10.7566/JPSCP.42.011023

First Results of an ATLASPix3.1 Telescope

Lingxin Meng[1], Attilio Andreazza[2], Daniel Muenstermann[1], Elisabeth Hutchinson[1], Fergus Wilson[3], Harald Fox[1], Ivan Peric[4], Jaap Velthuis[5], Jens Dopke[3], Juliette Martin[6], Ruoshi Dong[4,7], Riccardo Zanzottera[2], Rudolf Schimassek[4], Sam Moss[4], Shenghui Zeng[7,10], Tim Jones[8], Xiongxiong Xu[7,9], Yanyan Gao[6], Yiming Li[7], Yubin Zhong[1], Zirui Feng[5]

[1] *Lancaster University, UK,* [2] *INFN Milano, Italy,* [3] *RAL, UK,* [4] *KIT, Germany,* [5] *University of Bristol, UK,* [6] *University of Edinburgh, UK,* [7] *IHEP, China,* [8] *University of Liverpool, UK,* [9] *Tsinghua University, China,* [10] *South China University, China*

E-mail: lingxin.meng@cern.ch

(Received 20 January, 2023)

ATLASPix is a high-voltage CMOS pixel sensor designed as a candidate for the ATLAS ITk upgrade. Using a commercial 180 nm CMOS process, they are more cost-effective compared to hybrid pixel detectors. ATLASPix3.1 has an area of 2×2.1 cm^2, consisting of 150×50 μm^2 pixels, each with a large n-well as the charge collection electrode.
With the ability to be operated in a multi-chip setting for ATLAS ITk, LHCb or other future collider experiments, a 4-layer telescope made of ATLASPix3.1 was developed, using the GECCO readout system as for the single chip setup. To demonstrate the multi-chip capability and for its characterisation, a beam test was conducted at DESY using 3–6 GeV electron beam with the chips, arranged in a telescope and in a quad module, operated in triggerless readout mode with zero-suppression. In this proceedings we will present the first results of the ATLASPix3.1 beam telescope tested at the DESY testbeam.

KEYWORDS: ATLASPix, HVCMOS, MAPS, pixel, sensor, telescope, testbeam

1. Introduction

ATLASPix [1] is a high-voltage CMOS pixel sensor designed as a candidate for the ATLAS Inner Tracker (ITk) upgrade. Using the commercial ams/TSI 180 nm CMOS process, they are more cost-effective compared to hybrid pixel detectors. ATLASPix3 [2] is made on 200 Ωcm wafers and has an area of 2×2.1 cm^2 as shown in Fig. 1, being the first full reticle-sized sensor for the construction of multi-chip modules, like it is currently being carried out for the ATLAS ITk Pixel detector [3] or the LHCb Upstream Tracker upgrade [4]. The pixel matrix consists of 132 columns of 372 rows with 150×50 μm^2 pixels, which correspond to an active area of 1.98×1.86 cm^2. Each pixel has a large n-well as the charge collection electrode. The material budget is comparably low by using sensors thinned down to 150 μm.

Each pixel features a 3-bit trimming DAC (TDAC) for the trimming of the discriminator threshold, a 7-bit time-over-threshold (ToT) counter to measure the signal charge,

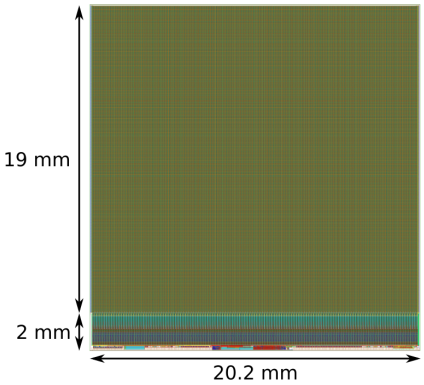

Fig. 1. Dimensions of the ATLASPix3.1 chip that consists of the pixel matrix on the top part and the periphery containing the readout logic located at the lower edge [5].

and a 10-bit time stamp recording the time-of-arrival of the detected hits. Calibrating the TDACs for fine-adjustment of pixel thresholds allows for a homogeneous detector response down to a threshold of 400 e.

Hits are read out through the column-drain architecture that can be operated in triggered or triggerless (hit-driven) mode. Output data use 8b10b line code in triggerless mode or 64b66b line code in triggered mode. Data are encoded using the Aurora protocol, providing RD53 [6] compatibility and an output bandwidth of up to 1.28 Gbit/s. To configure the chip, several interfaces are available: direct access to the signal pads, via SPI bus or a differential command line through command decoder.

The total power dissipation of the ATLASPix3 is 160 mW/cm^2, of which 120 mW/cm^2 are due to the analogue pixel circuitry. Compared to the power dissipation of the ATLAS ITk modules of 500 mW/cm^2, this reduces the required cooling power during operation. Due to the operation requirement from the ITk Pixel detector, voltage regulators are implemented to enable the chip to be operated in shunt-LDO mode in serial powering chains.

The changes from version 3 to version 3.1, which was delivered in 2021, incorporated a few improvements implemented through the metal layers, like biasing structure of the pixels, timewalk and voltage regulator circuit, but traded off shielding of the test signal injection, which results in crosstalk [5].

2. Test Setups

A single chip card (SCC), a quad module or a telescope can be read out using the GEneric Configuration and COntrol (GECCO) system. As can be seen in Fig. 2, the hardware is a Diligent Nexys Video FPGA board connecting to the GECCO board with function card slots. The GECCO board is attached either to an SCC (left) or a telescope adapter (right) that can host up to four SCCs at a 2.54 cm distance to each other. All telescope planes share the same bias voltage (HV) for the collection electrode and low voltages for the electronics, where the latter can be fine-tuned for each plane if regulators are used. The software provides a Qt-based graphical user interface to configure and calibrate the chip.

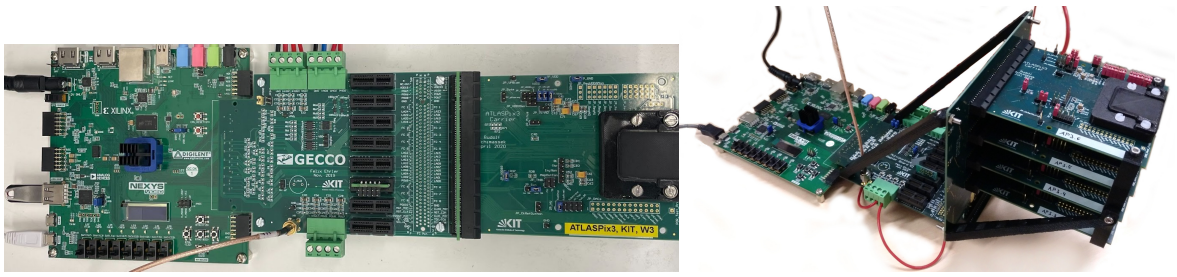

Fig. 2. The SCC setup (left) and the telescope (multi-chip) setup (right).

3. Laboratory Measurements

Before deployment in the testbeam, the sensors were characterised in the laboratory. IV curves were taken, the thresholds for each pixel were tuned and the response to radioactive sources was measured.

3.1 IV Curves

The leakage current as a function of the bias voltage of 12 ATLASPix3.1 chips is shown in Fig. 3. This measurement is to test the functionality of these chips that have been glued and wirebonded onto SCCs. Most of them break down at about 65 V as expected from the technology specifications, only two have early breakdowns.

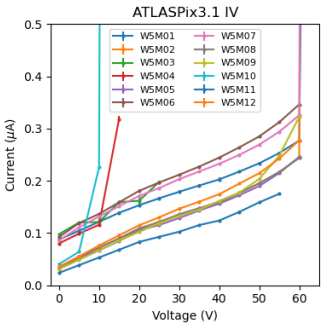

Fig. 3. IV curves from 12 ATLASPix3.1 chips, where the breakdown mostly occurs at 65 V.

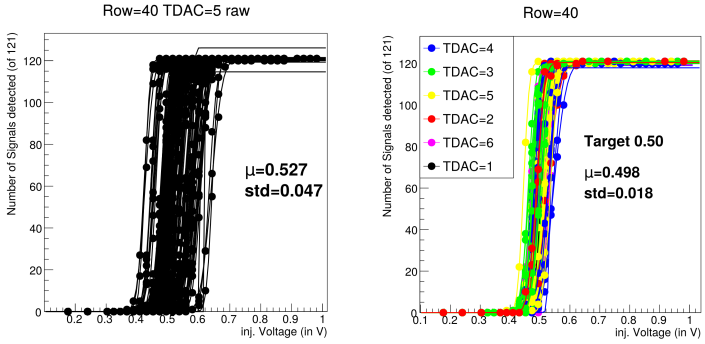

Fig. 4. S-curves from threshold scans of the 132 pixels in row 40 of an ATLASPix3 on an SCC before tuning (left) and after tuning (right). Before tuning the threshold distribution has $\sigma = 47$ mV, compared with $\sigma = 18$ mV after tuning.

3.2 Threshold Tuning

In addition to setting a global threshold for the whole pixel matrix, the threshold of individual pixels can be fine-tuned. Thus a uniform behaviour of all pixels within the same chip can be achieved. Fig. 4 shows scans (s-curves) around the discriminator threshold. The left and right plots compare between the untuned and tuned threshold, respectively, of the 132 pixels in row 40. With all TDACs at the same value of 5, the untuned threshold has a width of 47 mV, while after tuning, the TDACs take up different values and the distribution is narrowed down to 18 mV.

3.3 Source Scan

Ionising particles emitted by radioactive sources, such as Sr90, were recorded in the laboratory with the SCC setup. Fig. 5 (a) shows the response of a pixel matrix trimmed to a 0.5 V threshold during a 20 minute exposure time. The sensor was reverse-biased at 20 V. By varying the bias voltage, the depleted depth can be controlled. With increasing bias voltage, the depletion region becomes larger until the breakdown voltage of the CMOS process is reached. Thus more charge can be collected by the sensor, resulting in an increase of ToT and the number of hits registered. This can be seen in Fig. 5 (b), where the most probable value increases with increasing bias voltage.

3.4 Quad Module

Multi-chip modules consisting of four ATLASPix3 chips were built. The flexible printed circuit board (PCB) design, as shown in Fig. 6 (a), took inspiration from the ATLAS ITk pixel module. The chips are glued onto the PCB by hand where the chip periphery with the wirebond pads exceeds the flex on both sides, as shown in Fig. 6 (b). Source measurements with an x-ray tube were conducted. After an exposure time of 5 minutes at a rate of 15k–34k hits/s on chips with untuned threshold, the hitmap shown in Fig. 6 (c) is obtained. The areas with low numbers of hits (blue) correspond to SMD components on the flex shielding the x-ray. The areas with high numbers of hits (red) correspond to clearances around vias or cutouts in the flex.

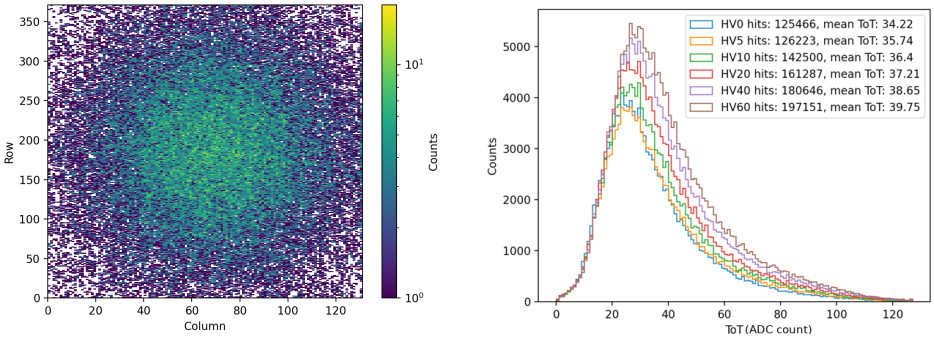

(a) (b)

Fig. 5. Source scan with Sr90. Left is the hitmap at a bias voltage of 20 V and on the right is the ToT distribution at different bias voltages ranging from 0 V to 60 V.

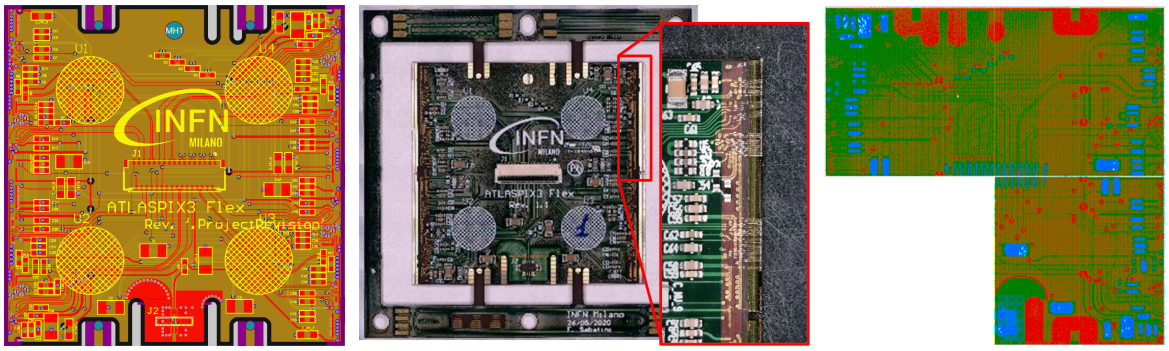

(a) (b) (c)

Fig. 6. (a) The quad PCB layout. (b) A quad module consisting of four ATLASPix3 chips assembled onto a flex PCB. The zoomed-in section shows details of the wirebonds. (c) A source scan with x-rays shows three out of four fully functioning chips. Red areas correspond to a high number of hits and blue corresponds to a low number of hits.

4. Testbeam at DESY

The testbeam campaign at DESY took place in April 2022, using a 3–6 GeV electron beam and two standalone telescope arms, each consisting of four SCC planes in the same orientation. Fig. 7 shows the two telescope arms with the planes interleaved. In this configuration, the telescope layers are at a distance of 1.27 cm from each other. At the bottom of the setup, the quad module is placed in a carrier in the beam. The ATLASPix3.1 sensors are biased at 50 V to ensure maximum depletion while staying below the breakdown voltage.

The two standalone telescope arms can be synchronised. This is achieved through the primary system providing the synchronisation signal to the secondary system, in order to reset the trigger ID and the time stamp counter. The hit-driven readout was used without any external trigger.

The first results shown below focus on data obtained from one of the telescope arms.

4.1 Reconstruction

Reconstruction and analysis are ongoing using the Corryvreckan [7] framework. For the reconstruction of the data taken with one telescope arm, layer 1, 2 and 4 are used as telescope planes. Layer

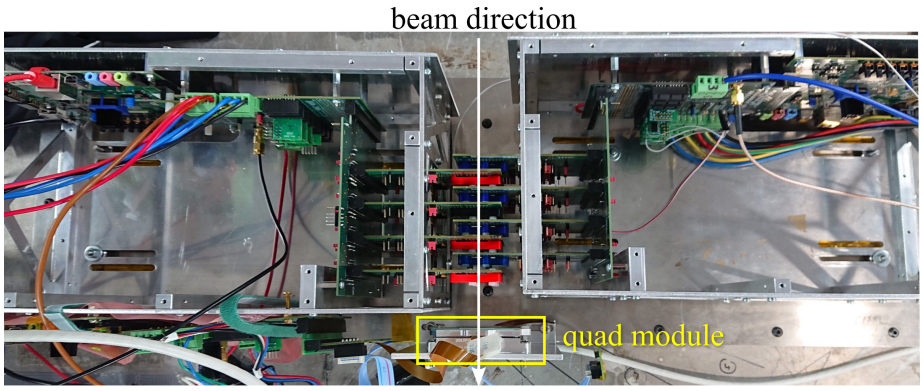

Fig. 7. Testbeam setup with two telescope arms interleaved. The beam enters from the top, traverses all eight layers and through the quad module mounted at the bottom.

3 is used as the device under test (DUT) plane. The layers 1–4 of each telescope arm are ordered from top to bottom on Fig. 7 with layer 1 being the first layer hit by the beam. Fig. 8 shows clusters on the DUT that are associated to reconstructed tracks. The beamspot is recognisable and agrees with observations during data taking. The correlations of the DUT plane with plane 1 in x- and y-directions are shown in Fig. 9. The clear correlations indicate that tracks are observed.

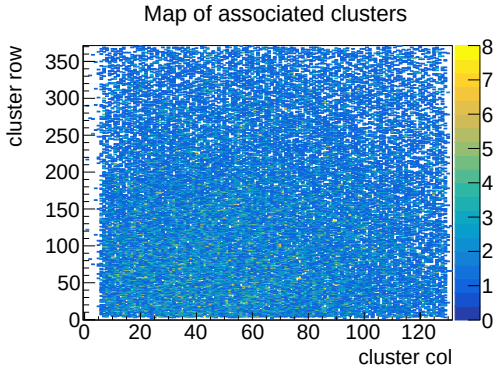

Fig. 8. Map of clusters on the DUT plane that are associated to a track.

4.1.1 Cluster Size and Charge Distribution

Fig. 10 shows the distributions of size (left) and charge (right) of clusters associated with a track. The cluster size distribution is dominated by single-pixel clusters. This is due to the large pixel size and small depletion depth compared to the size of charge cloud, thus lead to reduced charge sharing. The charge is measured as ToT which is in clock cycle units of 25 ns. As expected, the charge distribution follows the Landau shape.

4.1.2 Track-hit Residuals

The residual is defined as the position difference between a cluster and the interception of a reconstructed track with the plane of interest. For the testbeam data, the residual distributions for all planes are similar, showing the peak-structure as can be seen in Fig. 11 for the DUT plane. The peaks are more pronounced in the x-direction, along the long side (150 μm) of the pixel, but are also present

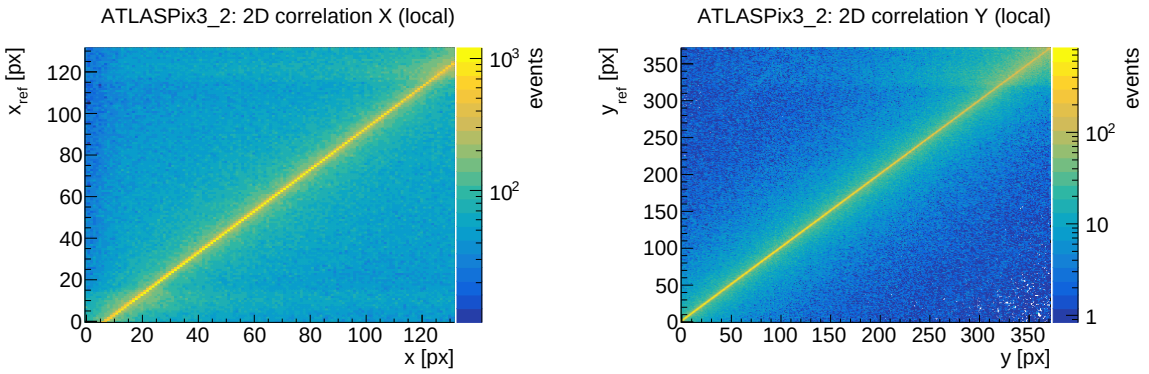

Fig. 9. X (left) and Y (right) correlations of the DUT with the reference plane.

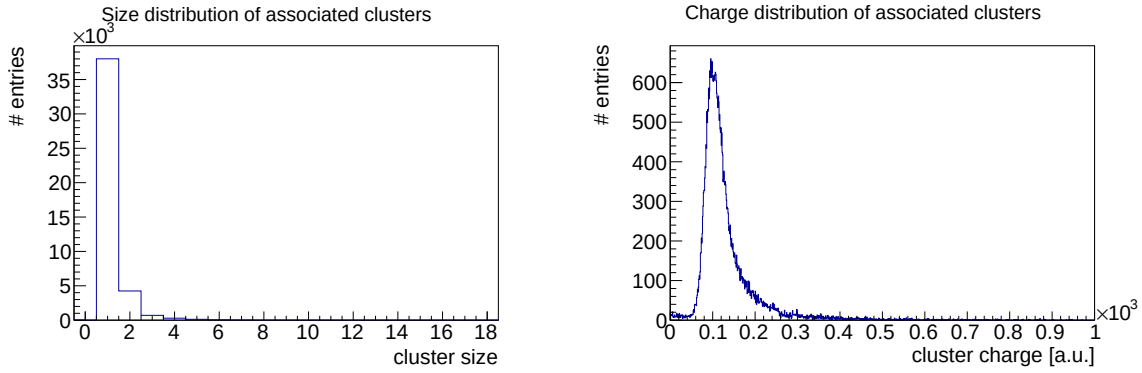

Fig. 10. Distribution of size (left) and charge (right) of DUT clusters associated to tracks.

in the y-direction, along the short side (50 µm) of the pixel.

The peak-structure is caused by the dominant portion of single-pixel-clusters as shown in Fig. 10. The beam is almost parallel and tracks are reconstructed using the centre location of these single-pixel clusters. For example, if a track traverses the same pixels on all planes but one, then the latter would acquire a quantised residual that is off by the distance of the pixel size.

Thus, the resulting tracking resolution would show discrete track positions within a pixel and cause the spiky residual distributions. To verify this behaviour, a simulation was run with the AllPix^2 [8] framework. The simulation can reproduce qualitatively the large fraction of single-pixel clusters, as shown in Fig. 12 (a). The resulting track-hit residuals in the DUT are shown in Fig. 12 (b) and (c) in x- and y-directions. They confirm qualitatively the behaviour observed in the data.

5. Conclusions

The full reticle-sized ATLASPix3.1 chips have been fabricated and successfully tested in the laboratory and at a testbeam at DESY using multi-chip assemblies: quad modules and four-layer telescopes. First results from reconstructed data of one telescope arm are shown and verified with simulations. Further analysis is ongoing.

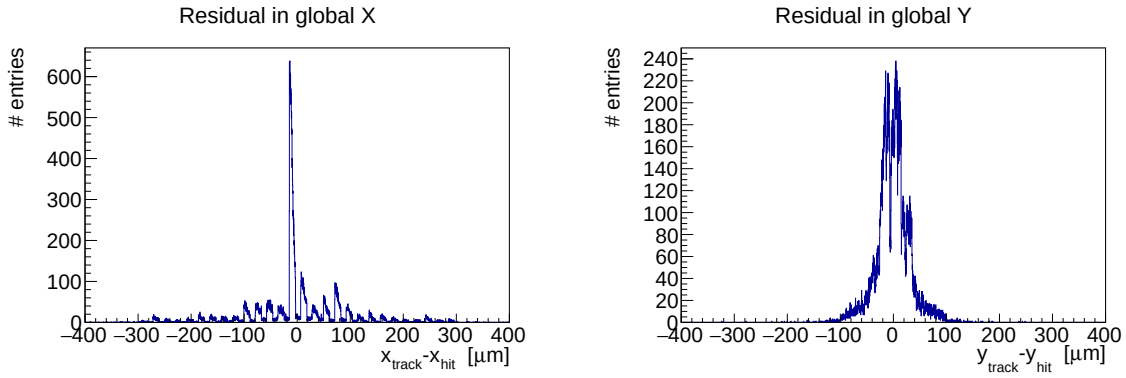

Fig. 11. Residual distributions in x- (left) and y-direction (right) from reconstructed data.

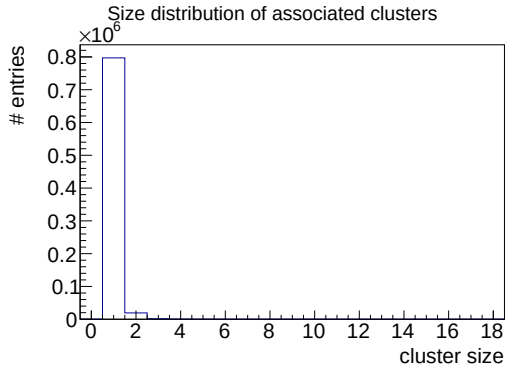

(a)

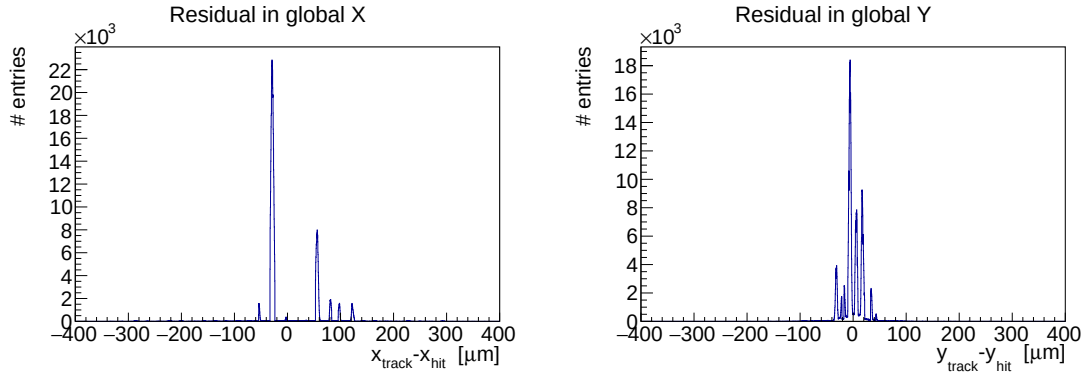

(b) (c)

Fig. 12. Simulated size distribution of clusters associated to a track (a), and x (b) and y (c) residual distributions.

6. Acknowledgements

The measurements leading to these results have been performed at the Test Beam Facility at DESY Hamburg (Germany), a member of the Helmholtz Association (HGF)

References

[1] I. Perić *et al*., IEEE Journal of Solid-State Circuits **56**, no. 8, p. 2488 (2021)
[2] R. Schimassek, Nucl. Instrum. Meth. A **986** 164812 (2021)
[3] L. Meng, PoS **TWEPP2019** 2020
[4] Y. Li, Nucl. Instr. Meth. A **1032** 166629 (2022)
[5] R. Schimassek, dissertation, DOI: 10.5445/IR/1000141412 (2021)
[6] A. Dimitrievska and A. Stiller, Nucl. Instr. Meth. A **958** 162091, (2020)
[7] D. Dannheim *et al.*, J. Instr. **16** P03008, (2021)
[8] S. Spannagel *et al.*, Nucl. Instr. Meth. A **901** (2018)